STRUCTURE OF HALOGENATES OF THE TYPE A $(BO_3)_2 \cdot H_2O$.

I. Barium Chlorate Monohydrate. Ba $(ClO_3)_2 . H_2O$

BY GOPINATH KARTHA

(Department of Physics, Indian Institute of Science, Bangalore)

Received September 6, 1952

(Communicated by Prof. R. S. Krishnan, F.A.SC.)

1. INTRODUCTION

A SERIES of compounds of the general type A $(BO_3)_2$, where A is a divalent metal and B a halogen, has been known for a long time, but a complete structure analysis of this type has not yet been undertaken. An important class of this type is the series of hydrated salts A $(BO_3)_2 . H_2O$ (Groth, 1908) many of which have been reported to be isomorphous. To this isomorphous series belong the crystals of Sr $(BrO_3)_2 . H_2O$; Ba $(ClO_3)_2 \cdot H_2O$; Ba $(IO_3)_2 . H_2O$; Pb $(ClO_3)_2 . H_2O$ and Pb $(BrO_3)_2 . H_2O$. The most common among these being Ba $(ClO_3)_2 \cdot H_2O$, a complete structure analysis of this crystal was undertaken.

The crystal structure data for halogenates in general are remarkably scarce. The structures of some unhydrated salts of monovalent metals which have the general formula ABO_3 have been analysed. They are found to have varying types of symmetry, from cubic to monoclinic depending on the elements A and B. In all the cases of chlorates and bromates studied, the BO_3^- ion has the same low pyramidal structure even though appreciable variation of bond lengths and angles might occur. Some of the iodates thus far studied do not show the low pyramidal configuration for the iodate ion, presumably due to the large crystal radius of the I^{+5} ion, *e.g.*, lithium iodate (Zachariasen and Barta, 1931) does not show separate iodate ions in the solid state, but each iodine atom is surrounded by six oxygen atoms each of which is equidistant from two iodine atoms. Hence we see a wide range of variation in the arrangement of atoms and the resultant symmetry in this type of crystals; and additional information regarding the structure of these crystals and the configuration of the halogenate ions and their variation from crystal to crystal would be welcome. The results of the analysis undertaken for the first crystal, *viz.*, barium chlorate monohydrate are presented in this paper.

The paper is divided into two parts. The first part deals with examination of morphological data, determination of the geometry and symmetry of the unit cell, the experimental procedure and the steps necessary to obtain a set of values for the various structure amplitudes on which the structure analysis is based. The second part deals with the use of these observed structure amplitudes in the actual determination of atomic parameters by two-dimensional Patterson and Fourier methods. A discussion of the proposed structure and an examination of the optical properties of the crystal based on it are included in the same part.

PART I

Experimental Details and Evaluation of Structure Amplitudes

2. MORPHOLOGICAL AND OPTICAL DATA

Barium chlorate monohydrate crystallises from a saturated aqueous solution in the form of needles elongated along the c-axis. The morphological studies (Eakle, 1896) showed the crystal to belong to the monoclinic prismatic class with axial ratios, $a:b:c = 1{\cdot}1416:1:1{\cdot}1981$ and monoclinic angle $\beta = 86°\,26'$. The m planes {110} are the most well developed. In most crystals neither {100} nor {010} faces were well developed. The optical data are:—strong positive birefringencc, optic axial plane (010), acute bisectrix makes with the c-axis an angle $23\frac{3}{4}°$ in the acute angle, the refractive indices are $\alpha = 1{\cdot}5622$, $\beta = 1{\cdot}5777$ and $\gamma = 1{\cdot}635$, and $2V = 55°\,30'$.

3. UNIT CELL AND SPACE GROUP

Using rotation and Weissenberg photographs, the unit cell dimensions and space group of the crystal have been determined (Kartha, 1951). The cell constants are: $a = 8{\cdot}86$ Å, $b = 7{\cdot}80$ Å, $c = 9{\cdot}35$ Å and $\beta = 93°\,30'$ and these agree well with the morphological data. The density of the crystal was found to be 3·18 gm. per c.c. and this gives the number of molecules per unit cell to be four. For this unit cell, the systematic absent reflections were hkl for $h + k + l$ odd; $hk0$ for $h + k$ odd and $h0l$ for either h or l odd. Since the crystal belongs to the monoclinic prismatic class, the space group is uniquely determined to be C^6_{2h}–I2/c. By a simple transformation of axes this can be brought to the orientation C2/c as given in the International Tables; but for the purpose of structure analysis the configuration I2/c which has unit cell constants nearest to that of a cube is preferred.

4. EXPERIMENTAL DETAILS

Filtered copper radiation was used for the determination of cell constants and space group. But, due to the very large value (approximately

570 cm.$^{-1}$) of the linear absorption coefficient of the crystal for CuKα radiation it was not possible to use this radiation in obtaining photographs for the purpose of making intensity estimates. Further, the scattering factor for barium is still large at the largest value of (sin θ/λ) obtainable with CuKα radiation, so that sufficient observational data could be obtained only by using a radiation of considerably smaller wave-length. Because of these reasons Mo radiation filtered through zirconium filter was used throughout for recording the reflections. Even though the linear absorption coefficient was still large, being about 70 cm.$^{-1}$ for Mo Kα radiation, the absorption errors could be reduced by using sufficiently small crystals and approximate absorption corrections.

The Weissenberg moving film method was used throughout for photographic recording, not only because indexing in that case would be easier, but especially due to the fact that the background intensity around the spots would be appreciably reduced. The spots were recorded by the multiple film method suggested by Robertson (1943) to increase the range of observed intensities. A batch of three films interleaved with silver foils of 0·001″ thickness was used. The absorption of the foil, film and two thicknesses of black paper together was found by microphotographic methods to reduce the intensity of spot from film to film by a factor of 2·5. Thus, assuming it to be possible to observe an intensity range of 1–100 in a single film, a range of intensities of 1--1600 could be thus obtained. The spots were indexed using the Buerger charts (Buerger, 1942) and the intensities were visually estimated by comparison with previously prepared standard set of intensity spots. Intensity estimates were obtained for each spot from all the three films and the mean, weighted in favour of the medium intensity spot was taken for further calculations.

The *c*-axis being the needle axis and the *m* planes being very well developed in most crystals the *hk*0 reflections were the easiest to obtain. For this, a crystal ground at the top to the form of a cylinder of radius 0·1 mm. leaving the crystallographic faces at the bottom clear was used. The crystal was set on an optical goniometer and the needle axis was made vertical, the reflections from the unground planes below being used to set the prism zones vertical. The crystal was then transferred to the Weissenberg camera without disturbing the setting and the zero level photograph was taken by the normal beam method. With the *a*- and *b*-axes, difficulties arose due to the fact that the crystal was rotated about an axis almost perpendicular to the needle axis. Here the heavy absorption by the crystal when either the incident or reflected beam is in the direction of the needle axis during rotation is liable to seriously affect the intensity values and accurate absorption

corrections will have to be applied if reliable data are to be expected. These corrections are tedious to calculate for a crystal whose section in the reflecting plane is not a circle. The inaccuracy due to neglecting a detailed absorption correction could be reduced by using the anti-equi-inclination method of recording the zero-layer with a large inclination angle. Then, in no position of the crystal during its rotation will the incident or the diffracted beam have to travel through the whole length of the needle axis. This technique was used for obtaining the $0kl$ and $h0l$ reflections.

5. CORRECTIONS FOR THE INTENSITIES

Once a set of relative intensities is obtained, the next step is to get a set of structure factors based on these assuming the intensities to obey the mosaic crystal formula. A number of corrections have to be made at this stage to the observed intensities, the nature of these corrections increasing in complexity and uncertainty when very accurate values are needed. But, for most purposes of structure analysis it is sufficient to make the most important corrections, *viz.*, Lorentz and polarisation corrections, as well as the absorption and temperature corrections.

The Lorentz and polarization corrections were made using the tabulated values of Buerger and Klein (1945) for the c-axis normal beam photograph and using the charts prepared by the author (Kartha, 1952) for the other two anti-equi-inclination photographs. In the case of the c-axis photograph, for which the crystal was ground in the form of a cylinder, the absorption correction was made following the method suggested by Bradley (1935) for cylindrical powder specimens. In the case of a- and b-axis photographs no absorption correction was made, but the errors arising from absorption were reduced by using a crystal of about 0·3 mm. cross-section and an anti-equi-inclination angle of 30°. The effect of neglecting the absorption correction is to increase the intensity of large angle reflections in comparison with those of smaller angles and in this respect it acts in a way opposite to that of the temperature factor, which has the effect of reducing the intensities of large angle reflections. This effect is considered in the next section.

6. THE SCALE AND TEMPERATURE FACTORS

If I is the intensity of the spot after making the above corrections, then it can be written in the form

$$I = k^2F^2T, \qquad (1)$$

where F is the structure amplitude of the reflection concerned, T is the temperature factor which is usually of the form exp. $[-B(\sin\theta/\lambda)^2]$ and k^2

is the factor which converts the observed intensities to an absolute scale. The scale factor k and the temperature factor B were determined by using the method of Wilson (1942). He has shown that in the case of a crystal with a large number atoms in the unit cell the relation

$$< | F_{hkl} | >_{av} = \frac{\Sigma_{hkl} | F_{hkl} |^2}{N} = \Sigma_r f_r^2 \qquad (2)$$

holds for a given angle of scattering, where f_r is the scattering factor of the atom r for the scattering angle under consideration and N is the number of reflections observed at this angle. Using equations (1) and (2) we have

$$< I >_{av} = k^2 \Sigma_r f_r^2 T = k^2 \Sigma f_r^2 \exp. [- B (\sin \theta/\lambda)^2]$$

Thus

$$\frac{\Sigma f_r^2}{< I >_{av}} = \frac{1}{k^2} \exp. [- B (\sin \theta/\lambda)^2]$$

and

$$\log \left\{ \frac{\Sigma f_r^2}{< I >_{av}} \right\} = B (\sin \theta/\lambda)^2 + \log k^2. \qquad (3)$$

Hence a graph with $\log (\Sigma f_r^2 / < I >_{av})$ as ordinate and $(\sin \theta/\lambda)^2$ as abscissa should be a straight line, the slope of which is B and the intercept on the y-axis is $\log k^2$, so that both the scale factor and the temperature factor can be obtained from the graph.

For each zone, the reflections were divided into groups having ranges $(\sin \theta/\lambda) \times 10^{-8}$: 0 — 0·2, 0·2 — 0·4, 0·4 — 0·6, 0·6 — 0·8, etc., and using the mean value of $(\Sigma f_r^2 / < I >_{av})$ for each range to correspond to the middle of the range, five or six points were obtained. All these points were found to fall approximately on a straight line, except the one for the smallest value of $(\sin \theta/\lambda)$, *viz.*, $0 \cdot 1 \times 10^8$ which was found to be appreciably above the average line. This was probably due to the large extinction effects occurring for these strong low angle reflections which reduce the value of I and thus lead to an abnormally large value of $\log (\Sigma f_r^2 / < I >_{av})$ in this region. Hence this point was neglected in drawing the graph from which the factors were read off.

By this method, values of $3 \cdot 2 \times 10^{-16}$, $1 \cdot 9 \times 10^{-16}$ and $1 \cdot 5 \times 10^{-16}$ were obtained for the constant B for the $hk0$, $h0l$ and $0kl$ reflections respectively. The small value of B for $0kl$ and $h0l$ reflections in comparison with that for the $hk0$ reflections is not surprising for the following reason. As mentioned in Section 6, the absorption correction was neglected for these two zones. The result of this is to effectively reduce the temperature factor as determined by the above method, in these cases.

Using the values of the scale factor k thus obtained the relative set of intensities were placed on an absolute basis to give values of $|F_{hkl}|$ for the various reflections. For the determination of atomic positions by Fourier synthesis, observed F-values uncorrected for temperature effect are preferable so as to avoid large termination errors. The temperature factors obtained by the above method were therefore used only for the comparison between observed structure factors and those calculated on the basis of the proposed structure. On an average an accuracy of 5–10% could be expected for the F_{hkl} values thus obtained, an accuracy which is satisfactory for most analyses.

PART II

Determination of Atomic Co-ordinates

7. Point Positions of Space Group I2/c

The symmetries of the space group I2/c are shown in Fig. 1, the usual nomenclature of International Tables being adopted. The general positions in the unit cell have a multiplicity of eight and the special positions on inversion centres or rotation axes number four. The equivalent point positions are shown in Fig. 2.

The point positions of multiplicity four are

(*a*)	0	0	0,	0	0	$\frac{1}{2}$,	$\frac{1}{2}$	$\frac{1}{2}$	$\frac{1}{2}$,	$\frac{1}{2}$	$\frac{1}{2}$	0
(*b*)	0	$\frac{1}{2}$	0,	0	$\frac{1}{2}$	$\frac{1}{2}$,	$\frac{1}{2}$	0	$\frac{1}{2}$,	$\frac{1}{2}$	0	0
(*c*)	$\frac{1}{4}$	$\frac{1}{4}$	$\frac{1}{4}$,	$\frac{3}{4}$	$\frac{3}{4}$	$\frac{1}{4}$,	$\frac{3}{4}$	$\frac{3}{4}$	$\frac{3}{4}$,	$\frac{1}{4}$	$\frac{1}{4}$	$\frac{3}{4}$
(*d*)	$\frac{1}{4}$	$\frac{3}{4}$	$\frac{1}{4}$,	$\frac{3}{4}$	$\frac{1}{4}$	$\frac{1}{4}$,	$\frac{3}{4}$	$\frac{1}{4}$	$\frac{3}{4}$,	$\frac{1}{4}$	$\frac{3}{4}$	$\frac{3}{4}$
(*e*)	0	y	$\frac{1}{4}$,	$\frac{1}{2}$	$\frac{1}{2}-y$	$\frac{1}{4}$,	$\frac{1}{2}$	$\frac{1}{2}+y$	$\frac{3}{4}$,	0	$\bar{y}$	$\frac{3}{4}$

and positions of multiplicity eight are

$$x \quad y \quad z, \quad \bar{x} \quad \bar{y} \quad \bar{z}, \quad \bar{x}\ y\ \tfrac{1}{2}-z; \quad x\ \bar{y}\ \tfrac{1}{2}+z$$
$$\tfrac{1}{2}+x \quad \tfrac{1}{2}+y \quad \tfrac{1}{2}+z, \quad \tfrac{1}{2}-x \quad \tfrac{1}{2}-y \quad \tfrac{1}{2}-z,$$
$$\tfrac{1}{2}-x \quad \tfrac{1}{2}+y \quad \bar{z}, \quad \tfrac{1}{2}+x \quad \tfrac{1}{2}-y \quad z,$$

The points listed in (*a*), (*b*), (*c*) and (*d*) have symmetry C_i and in (*e*) symmetry C_2.

8. Preliminary Considerations

Since there are four bariums, four water molecules and eight chlorate ions in the unit cell, we could normally expect the bariums and water oxygens to occupy special positions of multiplicity four and the chlorate

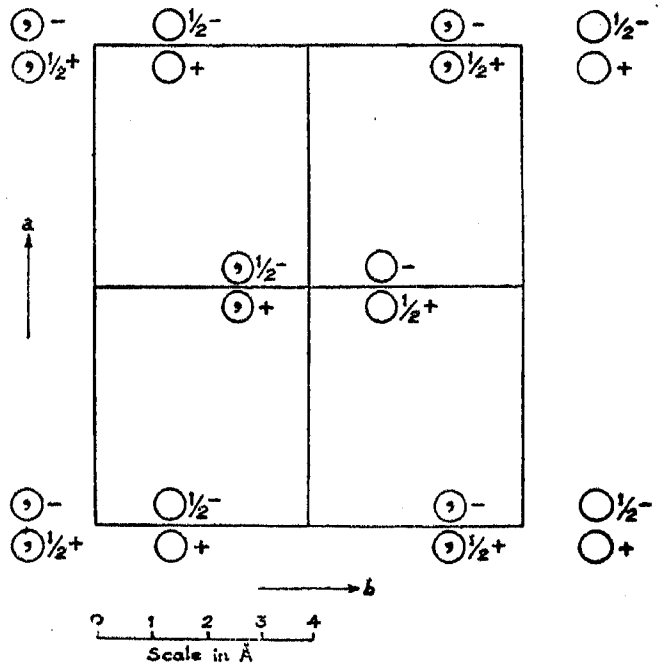

FIG. 1. Point positions in I 2*c*/ unit cell.

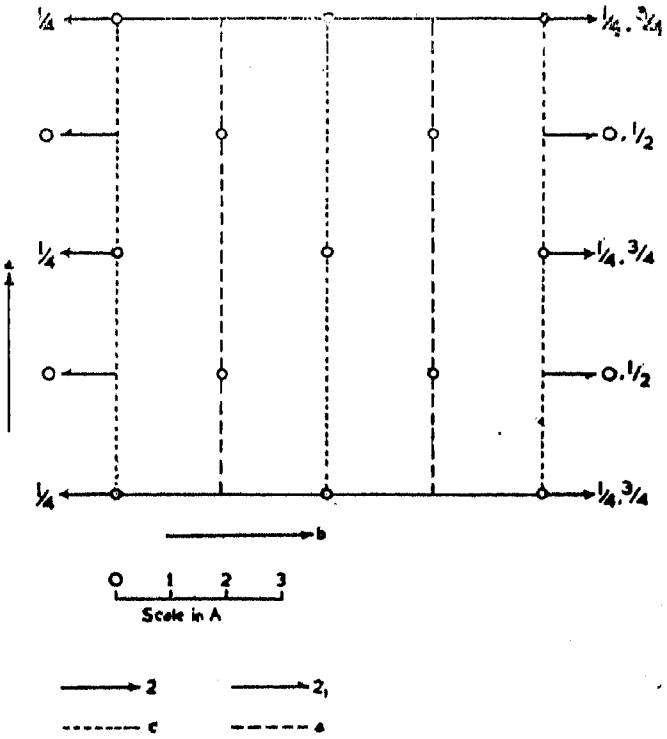

FIG. 2. Symmetries of unit cell I 2/*c*.

ion to occupy the general positions. It was observed that the set of reflections 4 0 0, 8 0 0, 12 0 0, 16 0 0 were very strong and exhibited

a normal decline of intensities. This suggests that the chlorine atoms lie very nearly midway between the (100) planes passing through the barium atoms which are at a distance of $a/2$ apart irrespective of which special positions they occupy. Now, two possibilities arise. The bariums may be either on one of the four sets of centres of inversion or they may be on the rotation axes. In the first case, the barium contribution for each $hk0$ reflection would be zero if h is odd, and a maximum if h is even. Hence we would expect on an average the h even reflections to be stronger than the h odd ones. No such regularity was observed and therefore the second alternative is more likely. However, a final decision can be arrived at only after a detailed examination of the complete intensity data.

9. THE c-AXIS PATTERSON PROJECTION

In the absence of any knowledge of the structural arrangement, the best use to which we can put the observational data is to make Patterson synthesis using the observed $|F_{hkl}|^2$ values in the series:

$$AP(u, v) = \sum_{h=-\infty}^{+\infty} \sum_{k=-\infty}^{+\infty} |F_{hk0}|^2 \exp.[(2\pi i (hu + kv)] \qquad (4)$$

For this space group (4) can be written in the form

$$AP(u, v) = \sum_{h=0}^{H} \sum_{k=0}^{K} |A_{hk0}|^2 \cos 2\pi hu \cos 2\pi kv, \qquad (5)$$

where H and K denote the maximum observed numbers for h and k and

$$|A_{000}|^2 = |F_{000}|^2 = |\Sigma Z_r|^2; \; |A_{h00}|^2 = 2|F_{h00}|^2$$
$$|A_{0k0}|^2 = 2|F_{0k0}|^2 \text{ and } |A_{hk0}|^2 = 4|F_{hk0}|^2$$

The series expressed in the form (5) is suited for calculation using the "Phasenfaktoren Tafel" (Beauclair, Sinogowitz, 1949). This book contains tables of functions $\cos 2\pi hx \cos 2\pi ky$ for h and k varying from 0–20 for points x, y in steps of 1/24. Calculations were first made using these tables but as the net obtained by this method was found to be too coarse for the contours to be drawn accurately, the Beevers-Lipson strip method (1936, *a*, *b*) was later used in evaluating the series. In this case the summation could be done in steps of 1/120 of the unit cell using the recent 3° one-dimensional Fourier strips. For this method of summing, the Fourier series (5) can be put in the more convenient form

$$AP(u, v) = \sum_{k=0}^{K} A(k, u) \cos 2\pi kv, \qquad (6)$$

where

$$A(k, u) = \sum_{h=0}^{H} |A_{hk0}|^2 \cos 2\pi hu. \qquad (7)$$

Values for the Patterson function P (u, v) are thus obtained at points on a rectangular net of side $a/120 = 0{\cdot}0738$ Å and $b/120 = 0{\cdot}0650$ Å. A quarter of the unit cell was covered by extending the summation for u and v from 0 to 0·500. In fact, by keeping $|A_{hk0}|^2$ terms with odd and even values of h and k separate during the summations, the summations need be carried out only in the range 0 to 0·250 for both u and v and the values for the rest of the unit cell could be obtained from these using the symmetry properties of the trigonometric functions and those of the space group under consideration. From the calculated P (u, v) values contours were drawn to show the distribution of the peaks of the Patterson function. The resulting map is shown in Fig. 3 in which only a quarter of the unit cell is drawn. The important peaks are marked in Fig. 4.

The peaks 1 and 1′ at (0, 0) and at $(\frac{1}{2}, \frac{1}{2})$ are of no interest, they being due to the nature of the function used and the space group. The peaks 2, 3, 4 being the most prominent, should enable one to fix the positions of bariums and chlorines in this projected unit cell; because, it is to be expected that the most prominent peaks would be those due to Ba—Ba, Ba—Cl or Cl—Cl vectors whose weights far outweigh those of the other possible vectors. Without any attempt to interpret all the peaks at this stage, though finally all the maxima should be explained in terms of the proposed structure, it is found that two sets of co-ordinates for barium and chlorine agree broadly

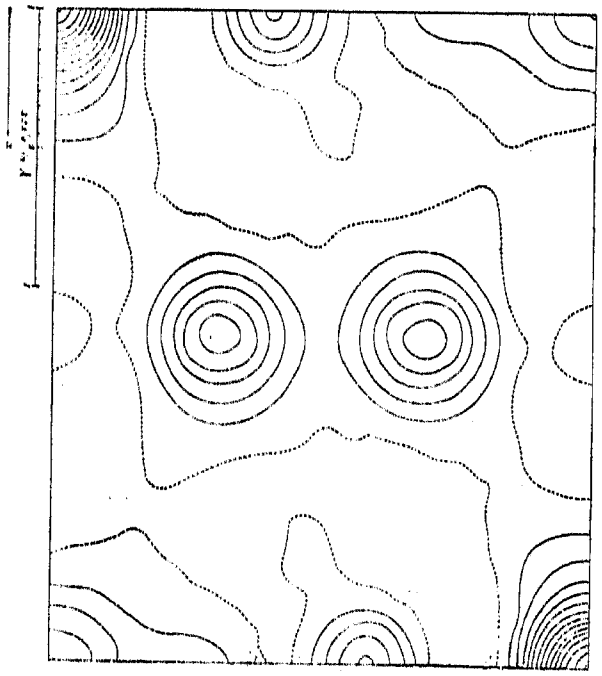

FIG. 3. Patterson projection on (001). Contours at intervals of 100 on an arbitrary scale.

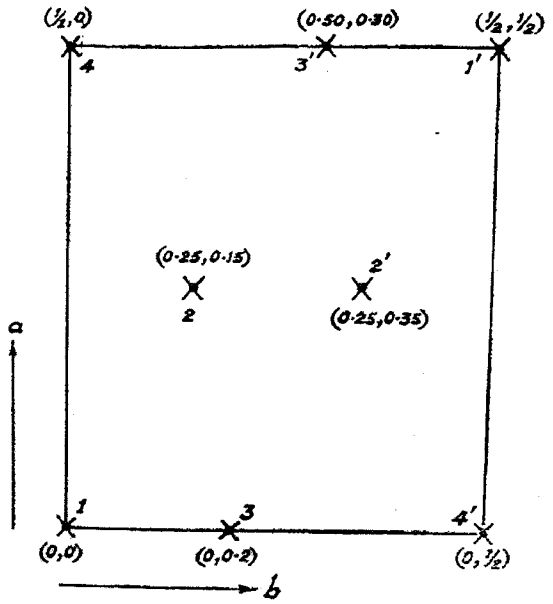

FIG. 4. Positions of Peaks in *c*-axis Patterson projection.

with the positions of the observed peaks, without considering their relative intensities. The two alternatives, one (I) in which a barium atom is at the centre of inversion and the other (II) in which it is on the rotation axis are diagrammatically shown in Figs. 5 and 6.

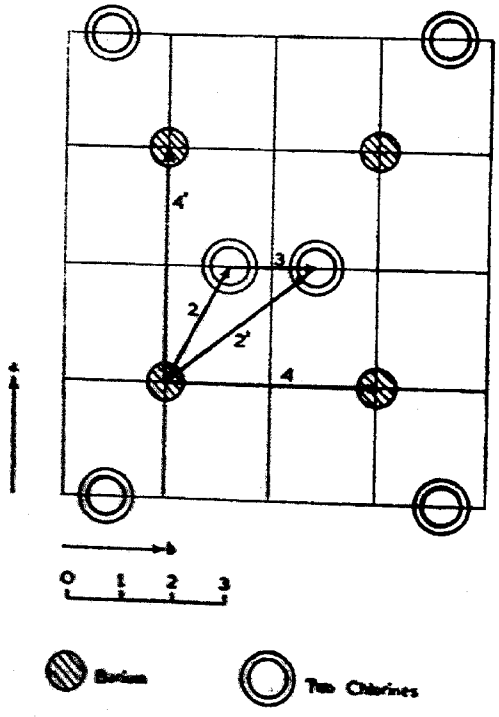

FIG. 5. Alternative I. Barium on centre of inversion.

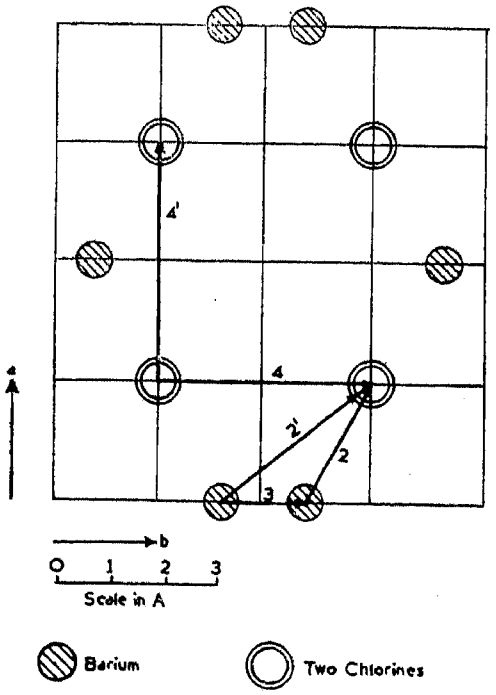

FIG. 6. Alternative II. Barium on rotation axis.

According to Fig. 5 where the barium is at a centre of inversion, the peak 3 corresponds to the superposition of eight Cl—Cl vectors and peak 4 to four Ba—Ba vectors, whereas according to Fig. 6, where barium is on a rotation axis, peak 3 corresponds to two Ba—Ba and peak 4 to sixteen Cl—Cl. Since the vector between atoms of scattering factors f_r and f_s has a weight $f_r f_s$, by putting approximate values for f_{Cl} and f_{Ba}, we find that according to alternative I, peak 4 should be about 4 times larger than peak 3, whereas according to alternative II they have about the same weight. Actually the projection showed that these peaks have approximately the same height. This again strengthens the guess made earlier that the bariums are situated on the rotation axes. In order to finally confirm this, Fourier syntheses were made according to both possibilities.

10. THE *c*-AXIS FOURIER PROJECTION

From the co-ordinates of the Patterson peaks two sets of atomic positions for barium and chlorine atoms are got for the above two alternatives. Assuming the co-ordinates of barium and chlorine to be x_1, y_1 and x_2, y_2 for the first case x_1', y_1' and x_2', y_2' for the second case, the following values are obtained for them:

I. $x_1 = 0{\cdot}25$ $\qquad$ $x_2 = 0{\cdot}50$

$\quad\;\; y_1 = 0{\cdot}25$ $\qquad$ $x_2 = 0{\cdot}40$

II. $x_1' = 0{\cdot}00$ $\quad x_2' = 0{\cdot}25$

$y_1' = 0{\cdot}40$ $\quad y_2' = 0{\cdot}25$

Since in the above considerations an origin chosen at a centre of inversion was used $F_{hk0} = \pm |F_{hk0}|$, *i.e.*, the sign alone will have to be determined for these reflections in order to perform the Fourier synthesis. The structure amplitudes for the various reflections could be split up into three parts and written as

$$F_{hk0} = F_{Ba} + F_{Cl} + F_0 \qquad (8)$$

the right-hand side denoting the barium, chlorine and oxygen contributions respectively to the structure amplitude. Now, the major part of the contribution to the scattering power of the unit cell is due to the barium and chlorine atoms whose co-ordinates are known to a good degree of accuracy from the Patterson projection, but for the ambiguity of the two alternatives. Thus, we can calculate the contributions $F_{Ba} + F_{Cl}$ to F_{hk0} and use the sign of the total contribution $F_{Ba} + F_{Cl}$ as the sign to be assigned to F_{hk0} in making the synthesis. Thus, using the two alternatives two sets of signs were obtained for the *hk*0 reflections. We could reasonably expect a very large percentage of the signs thus obtained to be correct if the correct alternative has been chosen. Two Fourier syntheses were made using in each case the observed magnitudes for the structure factors and the calculated signs by substituting these in the series:

$$\begin{aligned} A_{ab}\,\sigma(u, v) = F_{000} &+ 2\sum_{h=1}^{H} \pm |F_{h00}| \cos 2\pi hu \\ &+ 2\sum_{k=1}^{K} \pm |F_{0k0}| \cos 2\pi kv \\ &+ 4\sum_{h=1}^{H}\sum_{k=1}^{K} \pm |F_{hk0}| \cos \pi hu \cos 2\pi kv, \end{aligned} \qquad (9)$$

where $\sigma(u, v)$ is the electron density per unit area in the projected unit cell. The summations were made just as in the case of the Patterson projection and the contours were drawn.

From the two projections thus obtained it was found that the first alternative was untenable for three reasons:—(*a*) it showed almost the same value for the peaks of barium and chlorine, (*b*) it gave regions of very large negative electron density and (*c*) it showed no indications of the oxygen atoms. The second alternative, where bariums were assumed to be on rotation axes, gave reasonable values for barium and chlorine peaks and showed clearly resolved barium, chlorines and two oxygens in the quarter cell. The peaks of the chlorine atoms, however, left the other oxygen atoms unresolved. The water oxygens were not clearly resolved. Further details could be

obtained only after Fourier refinement and elimination of diffraction effects which are considered later in Section 14.

11. The *b*-Projection

A look at the space group extinctions for I2/*c* shows that all *h*0*l* reflections with either *h* or *l* odd are absent. This implies that in the *b*-projection both *a* and *c* are halved so that the projected unit cell has unit translations *a*/2 and *c*/2 and hence an area one-fourth of the unit cell. The projected unit cell contains one barium, two chlorines, six oxygens and one water oxygen. The scattering power of the barium atoms being much larger than that of any other atoms in the unit cell, the heavy atom method (Robertson and Woodward, 1936) could be used to obtain the Fourier projection. Further, since the barium atom is in a special position, it would project as a centre of inversion in the projected plane group irrespective of whether barium is on a rotation axis or a centre of inversion. For the sake of convenience this point could be taken as the origin in making this projection. (Since the barium is actually on the rotation axis this origin would be at a distance of 0·250 along the *c*-axis from the origin with respect to which the symmetries and point positions have been given earlier.) Thus the heavy barium atom being chosen at the origin which is also a centre of inversion for the plane group, it makes its full positive contribution for each reflection that is not absent on demands of space group. The contribution from barium far outweighs the effect of all other atoms and therefore completely determines the signs of the various reflections, which should therefore be positive throughout. Hence we can assume that $F_{h0l} = |F_{h0l}|$ in making the Fourier projection. This assumption was later justified for every reflection by calculation of the structure amplitudes using the contributions of all atoms in the unit cell.

For the *b*-projection we have the electron density given by

$$A_{ac}\,\sigma(u, w) = \sum_{l=0}^{L} A(l, u)\cos lw + \sum_{l=0}^{L} B(l, u)\sin lw, \tag{10}$$

where

$$A_{ac} = \text{Area of the projected unit cell}$$

$$A(l, u) = \sum_{h=0}^{H} A_{h0l}\cos 2\pi hu$$

$$B(l, u) = \sum_{h=0}^{H} B_{h0l}\sin 2\pi hu \tag{11}$$

$$A_{000} = F_{000};\quad A_{h00} = 2F_{h00}$$

$$A_{00l} = 2F_{00l};\quad A_{h0l} = 2\,[F_{h0\bar{l}} + F_{h0l}]$$

$$B_{000} = B_{h00} = B_{00l} = 0;\quad B_{h0l} = 2\,[F_{h0\bar{l}} - F_{h0l}]$$

The summations were made by the strip method and the final sums were multiplied by a suitable factor to give values directly in electrons per Å^2. The projection showed barium, chlorine and sixteen oxygen atoms resolved and indicated the pasitions of the other oxygen atoms. The water oxygen, which presumably is projected on top of the barium atom at the origin, is masked by the latter. The x and z co-ordinates were obtained from this projection and the structure factors for the various $h0l$ reflections were calculated. The calculations showed that all the assumed signs were correct and exhibited a remarkable agreement between the observed and calculated values, except for three very strong reflections of low (sin θ/λ) for which the observed values were too low. The obvious reason for this discrepancy was the neglect of absorption and extinction effects both of which tend to reduce the intensities of the strong low angle reflections.

12. THE a-AXIS PROJECTION

From the c- and b- axis projections, accurate values were obtained for all the co-ordinates of the heavier atoms and fairly good values for most of the oxygen co-ordinates. The other oxygen co-ordinates could not be so satisfactorily fixed due to the overlapping of the atoms in the projections. Since atoms which are unresolved in one projection might be clearly resolved in another, it was decided to make the a-projection also so that the best values for the various co-ordinates could be finally chosen. For this, the signs of the F_{0kl} were obtained by using the atomic co-ordinates got from the other two projections. Choosing the origin at $(00\frac{1}{4})$ so as to correspond to the earlier choices for the c- and b-projections, the structure factors are given by equations.

$$F_{0kl} = 0 \text{ for } k + l \text{ odd}$$

and

$$F_{0kl} = \sum_{r=1}^{6} 8 f_r \cos 2\pi k y_r \cos 2\pi l z_r \text{ for } k, l \text{ even}$$

$$F_{0kl} = \sum_{r=1}^{6} 8 f_r \sin 2\pi k y_r \cos 2\pi l z_r \text{ for } k, l \text{ odd} \qquad (12)$$

The signs got from these equations are used in the series

$$A_{bc}\,\sigma(v, w) \quad \sum_{k,\,l \text{ even}} \sum \pm |F_{0kl}| \cos 2\pi k v \cos 2\pi l w + \sum_{k,\,l \text{ odd}} \sum \pm |F_{0kl}| \sin 2\pi k v \cos 2\pi l w. \qquad (13)$$

This series was summed in the usual way using the Beevers-Lipson strips. The projection exhibited the important peaks, but it also showed very strong diffraction effects around the barium atoms which brought up spurious

peaks and cancelled some of the actual peaks. Hence oxygen positions could not be fixed with any degree of accuracy until this projection was refined and the diffraction effects were reduced.

13. Fourier Refinement of Projections

Having obtained, as described above, an approximate set of atomic co-ordinates, the projections were then refined to give more accurate co-ordinates. The signs of the various structure factors were recalculated using the atomic co-ordinates from the projection and the synthesis was performed with the new sets of signs. In the case of *c*-projection the first refinement revealed the position of the water oxygen also. For the *b*-projection the calculated F_{h0l}'s showed that no change was required in the assumed signs and hence this type of refinement was unnecessary in this case. But, there were a few reflections for which the observed intensities were too low for reasons explained before and the synthesis was therefore repeated using the calculated values (F_c) for these reflections. The effect of using F_c instead of F_0 for these few reflections is only to give zero weight for the observed values of these reflections and no great error is thereby introduced. Fourier refinement of *a*-projection did not improve it appreciably, owing to the enormous diffraction effects around the barium atoms. Hence further improvement of the projection could be done only after eliminating the diffraction effect which we shall consider next.

14. Elimination of Diffraction Effect

In the projections described in the previous section there are regions around the heavy atoms where appreciably large negative electron densities are found. This is to be attributed to the fact that the Fourier syntheses were performed using only reflections up to a $(\sin\theta/\lambda)$ range of about $0{\cdot}8 \times 10^8$ the coefficients of the higher terms in the Fourier series having been taken to be zero. Actually the scattering factors of barium and chlorine are still appreciable in the regions beyond $(\sin\theta/\lambda) = 0{\cdot}8\times10^8$. The effect of the termination of the Fourier series when the coefficients are still large is to introduce strong diffraction effects around the heavier atoms, which appear surrounded by a series of ripples of gradually diminishing amplitude. These rings of positive and negative electron density mask the peaks due to oxygen atoms in some cases and bring out spurious peaks. This difficulty was got over by extending the series as follows: Calculated F values (F_c) were used beyond the region for which F was observed, F_c being calculated from the contributions of only barium and chlorine atoms to the reflections. The positions of these are known very accurately because of two reasons, *viz.*, (1) The diffraction effects do not affect the positions of

maxima of the heavy atoms and (2) the co-ordinates of the heavy atoms could be accurately fixed from the Patterson projections where diffraction effects are negligible due to the large range of values used for the coefficients. The contribution of the oxygen atoms to the structure factor is very small for these large (sin θ/λ) values, because of the relatively faster decline of the atomic scattering factor with angle for oxygen. Further, the purpose of the extension of the Fourier series is to eliminate diffraction effects of the heavier barium and chlorine atoms. For these reasons, it is justifiable to use only the contributions of barium and chlorine atoms in calculating the structure factors F_c.

Thus the series was extended up to h, k, l values equal to twenty. Even then F_c values were not negligibly small and therefore a suitable temperature factor was used to reduce F_c values to a negligible amount beyond these regions. Of course, one could have used a large temperature factor without extending the series such that F values became very small even for (sin θ/λ) $= 0{\cdot}8\times10^{8}$; but this would certainly be detrimental to accuracy because of the accompanying broadening of the peaks. On the other hand, if the temperature factor is too small, the extension of the series will have to be made to such large values of h, k and l that computation would be very laborious. The final choice of the temperature factor B was a compromise between the two opposing considerations. The B values chosen were $3{\cdot}2\times10^{-16}$ for b- and c-projections and $4{\cdot}0\times10^{-16}$ for the a-projection. In the case of projections where the value of the temperature factor used was larger than that actually found, the observed structure factors were multiplied by a suitable factor so as to bring all the F values (both F_0 and F_c) used for a particular summation to have the same effective temperature factor. Using the series thus extended, the projections were made.

15. FINAL PROJECTIONS

The final projections obtained after refinement and elimination of diffraction effects are shown in Figs. 7 to 12 together with their key diagrams. These projections were found to be largely free from the diffraction effects. The atomic co-ordinates obtained from them could explain all the peaks in the Patterson projections shown in Figs. 3 and 13.

16. ATOMIC CO-ORDINATES

All the three projections together with the Patterson diagrams fixed the barium and chlorine positions to an accuracy of $\pm 0{\cdot}002$ of the unit cell dimensions. Some of the oxygen atoms, though resolved in one projection, were found overlapping with the heavier atoms in another projection

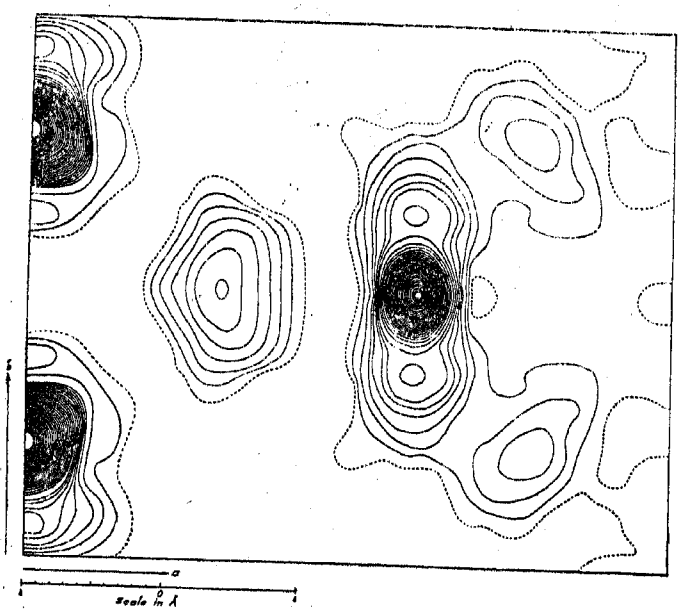

FIG. 7. Final (100) F-projection. Contours at intervals of 2 e. per Å^2 around oxygen, & 4 elsewhere.

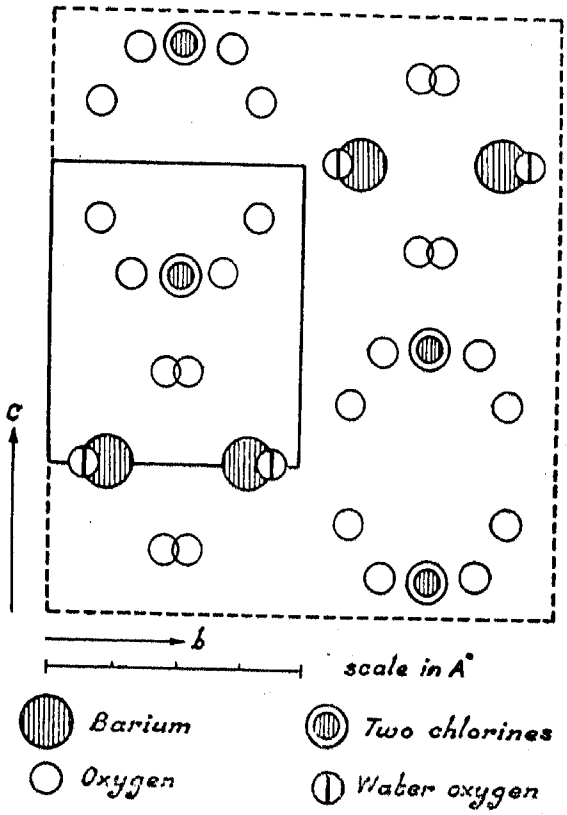

FIG. 8. Atomic positions in *a*-projection.

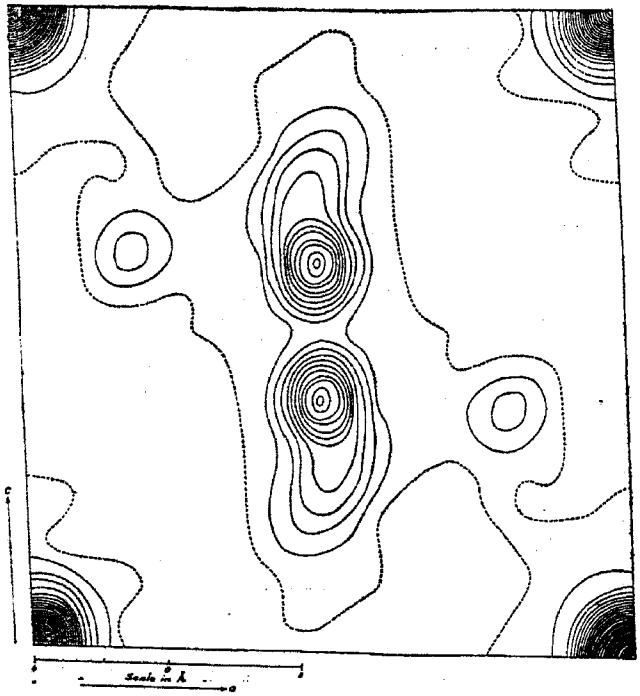

FIG. 9. Final (010) Fourier projection after minimising diffraction errors also. Contours at intervals of 4 electrons per Å².

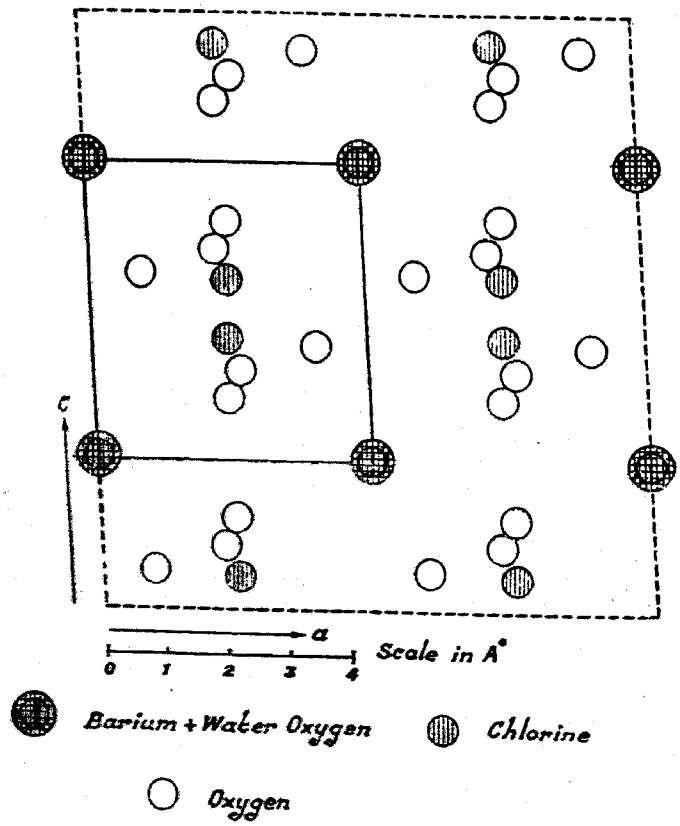

FIG. 10. Atomic positions in *b*-projection.

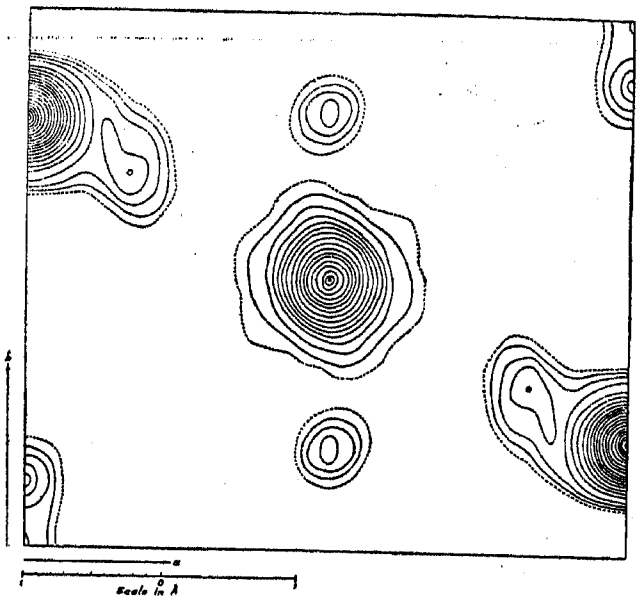

FIG. 11. Final (001) F-projection using F_c values also in synthesis to eliminate diffraction effects. Contours at intervals of 2 *e*. Å^2 around oxygen and 4 *e*, Å^2 elsewhere.

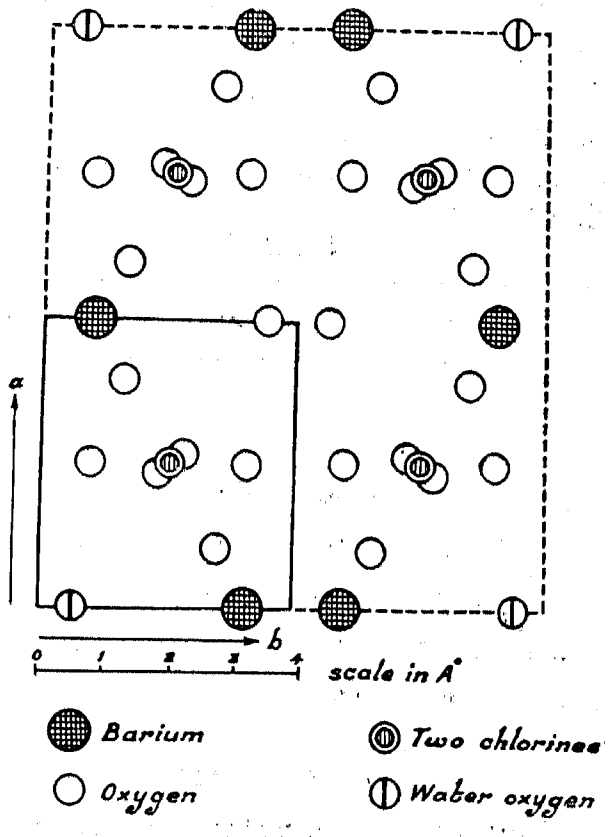

FIG. 12. Atomic positions in *c*-projection.

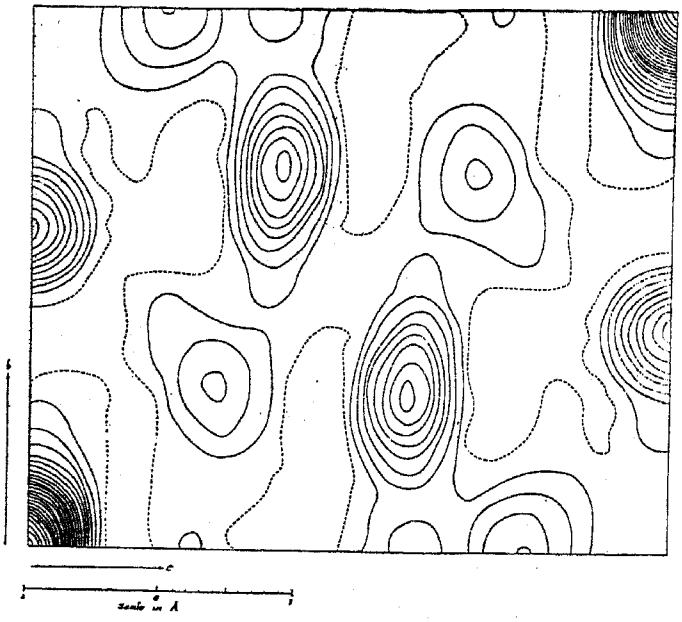

FIG. 13. Patterson projection on (100). Contours at intervals of 50 on an arbitrary scale.

so that the best set of values from all the three projections was finally chosen for these atoms. Due to the comparatively small scattering contribution of the oxygen atoms to the various reflections an accuracy not much better than 0·005 could be expected for the oxygen co-ordinates. The final table of co-ordinates, both fractional and in angstroms, are presented in Table I; the co-ordinates being given with respect to the origin of the space group as given in Section 8.

TABLE I

Atom	Fractional Co-ordinates			Co-ordinates in angstroms		
	u	v	w	x	y	z
1 Barium ..	0·000	0·396	0·250	0·00	3·09	2·34
2 Chlorine ..	0·250	0·250	0·554	2·22	1·95	5·18
3 Oxygen 1 ..	0·092	0·342	0·562	0·82	2·67	5·25
4 Oxygen 2 ..	0·254	0·096	0·650	2·25	0·75	6·08
5 Oxygen 3 ..	0·267	0·225	0·396	2·37	1·76	3·70
6 Water Oxygen ..	0·000	0·062	0·250	0·00	0·48	2·34

17. ACCURACY

The validity of any proposed structure must on the final analysis rest on the agreement between the structure amplitudes F_c calculated on the

TABLE II. *Observed and Calculated Structure Amplitudes*

h	*k*	*l*	$F_{calc.}$	$F_{obs.}$	*h*	*k*	*l*	$F_{calc.}$	$F_{obs.}$
0	0	0	592	..	9	1	0	−52	57
0	2	0	− 74	98	9	3	0	37	37
0	4	0	− 74	85	9	5	0	54	55
0	6	0	−143	135	9	7	0	6	0
0	8	0	74	57	9	9	0	−36	39
0	10	0	23	30	10	0	0	34	40
0	12	0	21	0	10	2	0	48	45
0	14	0	− 28	26	10	4	0	−77	67
1	1	0	−165	166	10	6	0	− 1	0
1	3	0	107	128	10	8	0	− 2	0
1	5	0	134	137	10	10	0	29	32
1	7	0	− 3	0	11	1	0	−41	42
1	9	0	− 57	46	11	3	0	24	22
1	11	0	− 26	27	11	5	0	43	42
1	13	0	16	16	12	0	0	84	87
2	0	0	45	30	12	2	0	− 9	0
2	2	0	162	186	12	4	0	−20	18
2	4	0	−191	199	13	1	0	−31	30
2	6	0	3	0	13	3	0	18	19
2	8	0	− 9	0	13	5	0	28	29
2	10	0	63	42	14	0	0	14	0
2	12	0	− 16	0	14	2	0	23	27
3	1	0	−106	79	14	4	0	−34	40
3	3	0	51	60	15	1	0	−16	19
3	5	0	113	130	15	3	0	6	0
3	7	0	3	0	15	5	0	21	26
3	9	0	− 56	43	16	0	0	31	27
3	11	0	− 27	25	0	0	2	124	90
3	13	0	17	0	0	0	4	133	131
4	0	0	291	290	0	0	6	190	180
4	2	0	− 13	27	0	0	8	66	60
4	4	0	− 56	50	0	0	10	142	119
4	6	0	−144	146	0	0	12	52	39
4	8	0	63	47	0	0	14	49	46
4	10	0	25	42	0	0	16	50	51
4	12	0	17	0	2	0	0	44	21
5	1	0	− 85	67	2	0	2	296	203*
5	3	0	33	35	2	0	4	180	138
5	5	0	93	98	2	0	6	137	111
5	7	0	18	0	2	0	8	139	130
5	9	0	− 54	45	2	0	10	46	44
5	11	0	− 21	19	2	0	12	69	87
6	0	0	13	0	2	0	14	48	35
6	2	0	105	89	2	0	16	38	30
6	4	0	−119	101	4	0	0	302	172*
6	6	0	− 16	32	4	0	2	123	120
6	8	0	− 4	0	4	0	4	104	95
6	10	0	54	36	4	0	6	144	141
7	1	0	− 63	55	4	0	8	71	58
7	3	0	23	27	4	0	10	104	87
7	5	0	80	81	4	0	12	56	37
7	7	0	2	0	4	0	14	48	39
7	9	0	− 41	42	4	0	16	37	35
8	0	0	158	140	6	0	0	13	0
8	2	0	− 18	0	6	0	2	196	149
8	4	0	− 29	25	6	0	4	134	128
8	6	0	− 86	74	6	0	6	65	65
8	8	0	44	39	6	0	8	124	135
					6	0	10	36	25

TABLE II—(*Contd.*)

h	*k*	*l*	$F_{calc.}$	$F_{obs.}$	*h*	*k*	*l*	$F_{calc.}$	$F_{obs.}$
6	0	12	60	60					
6	0	14	48	39	4	0	$\overline{16}$	44	30
8	0	0	182	168					
8	0	2	47	55	6	0	$\overline{2}$	180	150
8	0	4	103	118					
8	0	6	95	96	6	0	$\overline{4}$	138	131
8	0	8	44	39					
8	0	10	93	79	6	0	$\overline{6}$	92	81
8	0	12	37	30					
10	0	0	42	37	6	0	$\overline{8}$	129	132
10	0	2	106	116					
10	0	4	76	67	6	0	$\overline{10}$	32	39
10	0	6	52	51					
10	0	8	71	67	6	0	$\overline{12}$	83	115
10	0	10	29	20					
10	0	12	38	30	6	0	$\overline{14}$	54	39
12	0	0	110	120					
12	0	2	27	14	6	0	$\overline{16}$	26	25
12	0	4	49	60					
12	0	6	66	63	8	0	$\overline{2}$	96	78
12	0	8	20	14					
12	0	10	51	60	8	0	$\overline{4}$	73	67
14	0	0	20	21					
14	0	2	69	78	8	0	$\overline{6}$	104	119
14	0	4	34	25					
14	0	6	30	30	8	0	$\overline{8}$	54	76
16	0	0	51	46					
16	0	2	21	21	8	0	$\overline{10}$	91	98
					8	0	$\overline{12}$	44	39
2	0	$\overline{2}$	216	168*					
2	0	$\overline{4}$	260	189	8	0	$\overline{14}$	40	35
2	0	$\overline{6}$	124	81	10	0	$\overline{2}$	95	113
2	0	$\overline{8}$	139	134	10	0	$\overline{4}$	77	88
2	0	$\overline{10}$	60	49	10	0	$\overline{6}$	72	74
2	0	$\overline{12}$	80	78	10	0	$\overline{8}$	76	79
2	0	$\overline{14}$	48	42	10	0	$\overline{10}$	27	55
2	0	$\overline{16}$	37	25	10	0	$\overline{12}$	62	87
4	0	$\overline{2}$	128	98	10	0	$\overline{14}$	31	34
4	0	$\overline{4}$	140	112	12	0	$\overline{2}$	45	37
4	0	$\overline{6}$	127	123	12	0	$\overline{4}$	60	71
4	0	$\overline{8}$	98	100	12	0	$\overline{6}$	56	81
4	0	$\overline{10}$	129	112	12	0	$\overline{8}$	32	39
4	0	$\overline{12}$	44	27	12	0	$\overline{10}$	69	65
4	0	$\overline{14}$	55	42	12	0	$\overline{12}$	22	25

TABLE II—(*Contd.*)

h	k	l	$F_{calc.}$	$F_{obs.}$	h	k	l	$F_{calc.}$	$F_{obs.}$
					0	6	2	−56	40
14	0	$\bar{2}$	50	70	0	6	4	−59	49
					0	6	6	−61	56
14	0	$\bar{4}$	54	60	0	6	8	−29	33
					0	8	0	67	48
14	0	$\bar{6}$	38	25	0	8	2	3	15
					0	8	4	31	26
14	0	$\bar{8}$	48	58	0	1	3	181	154
					0	1	5	11	5
6	0	$\bar{2}$	32	25	0	1	7	131	132
0	0	2	124	88	0	1	9	38	23
0	0	4	133	120	0	1	11	5	7
0	0	6	190	167	0	3	1	137	111
0	0	8	66	35	0	3	3	129	118
0	0	10	142	111	0	3	5	199	159
0	2	0	− 71	83	0	3	7	52	31
0	2	2	156	131	0	3	9	64	66
0	2	4	55	48	0	5	1	5	0
0	2	6	− 13	20	0	5	3	14	13
0	2	8	64	74	0	5	5	34	24
0	2	10	− 2	12	0	5	7	24	20
0	4	0	− 75	60	0	5	9	−10	10
0	4	2	−161	123	0	7	1	−64	60
0	4	4	− 93	76	0	7	3	−95	76
0	4	6	− 55	37	0	7	5	−44	51
0	4	8	− 85	88	0	7	7	−76	62
0	4	10	− 33	31	0	9	1	−28	12
0	6	0	−134	91	0	9	3	0	8

basis of the structure and the values F_0 obtained experimentally. To show the extent of agreement between the observed and calculated values the two sets are given in Table II. The F_0's marked with asterisks are the $h0l$ reflection for which F_c is far greater than F_0 due to the absorption and extinction effects as mentioned earlier.

As a measure of the agreement between the calculated and observed structure amplitudes the function

$$R = \Sigma \Big| |F_0| - |F_c| \Big| \Big/ \Sigma |F_0|$$

was calculated for the various projections separately and finally for all the reflections taken together, with the results given in Table III.

The function R′ given by $\Sigma \Big| |F_0| - |F_c| \Big| \Big/ \Sigma |F_c|$ had a mean value 0·165, as against 0·178 for R. Unobserved reflections in these ranges of $(\sin\theta/\lambda)$ were also taken in calculating the reliability indices R and R′.

TABLE III

Projection	$(\sin\theta/\lambda)$ range up to which comparison was made	Number of reflections compared	R
a	$0{\cdot}70\times10^8$	46	0·21
b	$0{\cdot}95\times10^8$	109	0·16
c	$0{\cdot}85\times10^8$	86	0·178
Combined	..	241	0·178

As is to be expected, the agreement is best for the *b*-projection where the largest $(\sin\theta/\lambda)$ range and the maximum number of reflections were used; and the least for the *a*-projection where the smallest number of reflections was used and no absorption corrections were made. On the whole, the agreement can be considered to be good especially because the structure determination has been based only on projections 8–9 Å deep. Of course, part of the value of R will be due to errors in measured F values and to neglect of corrections, but a major part must be attributed to the lack of spherical symmetry in the atomic electronic distribution in the crystal and due to the presence of hydrogen atoms whose existence has not been taken into account in calculating the F_c values.

18. DISCUSSION OF THE STRUCTURE

There are eight chlorate ions in the unit cell all of which are obtained from a single ion by the operations of screw axes and inversions. The general arrangement of atoms is shown in Fig. 14 which gives a perspective diagram of the unit cell.

The chlorate ions remain as independent units having the usual distorted low pyramidal structure with an oxygen triangle of average side 2·52 Å and chlorine-oxygen distance 1·57 Å. The chlorine atom is at a distance of 0·45 Å from the oxygen plane. It is interesting to compare these values with the values for the chlorate ions in the case of sodium chlorate and potassium chlorate crystals (Zachariasen, 1929) and these together with the corresponding values for barium chlorate are given in Table IV.

Each chlorine atom is linked to four barium atoms and each barium to eight chlorines at an average distance of 3·89 Å. There is also a barium atom in a line almost normal to the oxygen plane of a chlorate ion at a distance of 5·76 Å from the chlorine. The barium atom is surrounded by ten

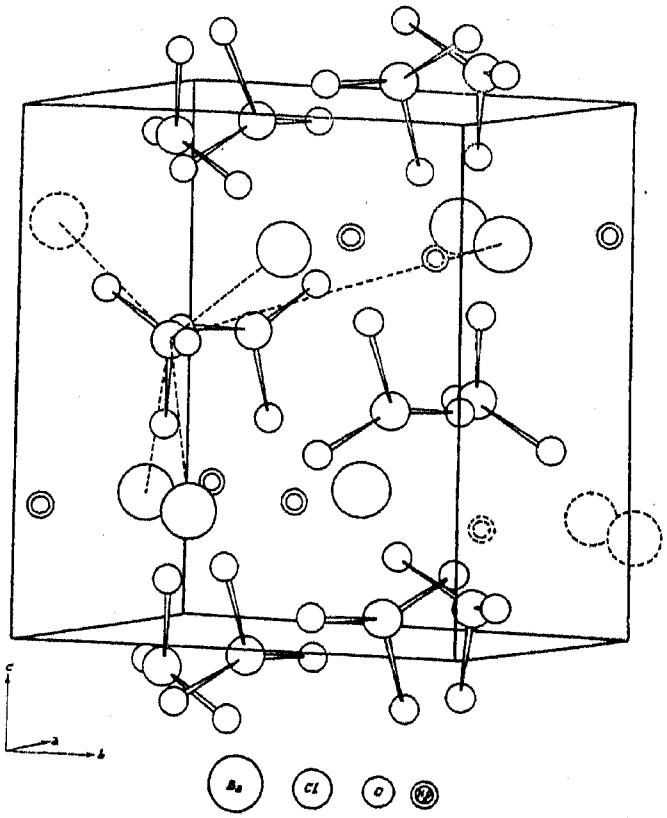

FIG. 14. Barium chlorate monohydrate.

TABLE IV

Crystal		Oxygen–Oxygen	Chlorine–Chlorine	Displacement of Cl atom from O_3 plane
Sodium Chlorate ..	Zachariasen	3*a*, 2·38 Å	1·48 Å	0·48 Å
Potassium Chlorate ..	do	1*a*, 2·48 Å	*a* 1·60 Å	0·50
		2*b*, 2·33 Å	2*b*, 1·42 Å	
		Mean = 2·43 Å	Mean = 1·48 Å	
Barium Chlorate ..	Author	*a*, 2·52 Å	*a*, 1·60 Å	0·45 Å
		b, 2·59 Å	*b*, 1·51 Å	
		c, 2·45 Å	*c*, 1·59 Å	
		Mean = 2·52 Å	Mean = 1·57 Å	

oxygen atoms at a mean distance of 2·87 Å and by a water oxygen on the rotation axis at a distance of 2·60 Å. This average barium-oxygen distance

2·87 Å is slightly greater than the value 2·75 Å given as the sum of crystal radii for Ba^{++} and O^{--} (Pauling, 1948). The various interatomic distances are collected in Table V.

TABLE V

Atoms	Cl—O	O—O	Ba—O	Ba-Water Oxygen
	..	..	3·02	
	1·60	2·52	2·97	
Distance in Å ..	1·51	2·59	2·78	2·60
	1·59	2·45	2·74	
	..	..	2·84	
Mean ..	1·57 Å	2·52 Å	2·52 Å	2·60 Å

19. OPTICAL PROPERTIES

We shall now consider the explanation of the strong positive birefringence of the crystal on the basis of this structure. The optical properties of the crystal are summarised in Fig. 15.

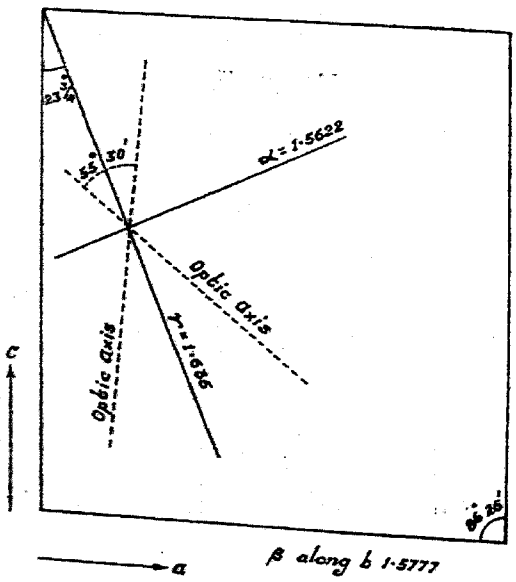

FIG. 15. Optical constants of barium chlorate.

It is well known that a flat molecule, or a polyatomic ion in which all atoms lie in a plane, has a higher refractive index when the electric vector lies in the plane of the group of atoms than when it is perpendicular to the plane. In crystals these ions are surrounded by others and the interaction

between them introduces complication, but the distances between atoms in the neighbouring molecules are in general much greater than those linked by direct bonds. Since the induction effects fall off rapidly with increasing distance, the interaction between different molecules may be neglected as a first approximation. Hence the main factor contributing to the birefringence of crystals containing strongly anisotropic ions is the relative orientation of these units. When they are all parallel as in the case of most nitrates and carbonates the anisotropy is almost the same as that of the units; but when these units are inclined to each other in the unit cell their individual effects cancel out particularly, or sometimes completely as in cubic crystals. When such ions have their planes inclined at an appreciable angle to each other but are all parallel to a line, the refractive index along this line will be high, but in other directions it will be comparatively low corresponding to an average value for the other two principal directions of the molecule and hence the birefringence would be positive. These ideas enable one to explain the optical properties of barium chlorate from the orientations of the chlorate ions in the unit cell as indicated below.

In barium chlorate, the bulk of the contribution to the refractivity is from the chlorate ions, in particular from the O_3 groups. The planes of these groups have only two types of orientations in the crystal, the two being related to each other by a rotation of 180° about the *b*-axis. If we denote by *l*, *m*, *n* the direction cosines of the normals to the two types of oxygen planes with reference to the co-ordinate axes parallel to *b*, *c* and the third mutually perpendicular direction, then it can be shown that they have the following values for the structure determined here

$$l = 0{\cdot}674 \qquad m = 0{\cdot}652 \qquad n = 0{\cdot}348$$

$$l = 0{\cdot}674 \qquad m = -0{\cdot}652 \qquad n = 0{\cdot}348$$

Thus the line of intersection of the two planes (*i.e.*, common direction to the oxygen planes) lies in the *a*-*c* plane (Fig. 16). If A is the angle made by this line with the *c*-axis, then $\cot A = l/n = 1{\cdot}937$, so that $A = 27° 18'$. Thus the common direction makes an angle approximately 27° with the *c*-axis in the acute angle between *c* and *a*. Being a direction common to the two O_3 groups, this will be the direction of maximum refractive index (γ). Further, the normal to the oxygen planes of the chlorate ions make an angle $\theta = \cos^{-1} m = 49° 17'$ with the *b*-axis and this angle remains the same for all the ions. Thus the angle made by the oxygen planes with the *b*-axis is smaller than 45°, and hence the refractive index along the *b*-direction will be the larger of the two smaller refractive indices (α and β).

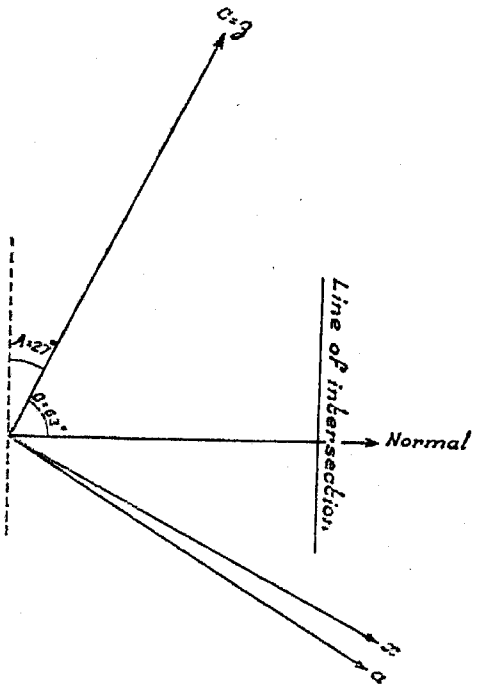

FIG. 16. Line of intersection of oxygen plane and (010) plane.

To summarise, the structure enables us to predict the following: (1) The largest refractive index (γ) will be in a direction making an angle $A = 27°$ with the c-axis. (2) The middle refractive index (β) will be along the b-direction and β will be nearer to α than to γ. These are in agreement with the observed data $\alpha = 1{\cdot}5622$, $\beta = 1{\cdot}5777$, $\gamma = 1{\cdot}635$ and $A = 23\frac{3}{4}°$.

In conclusion, the author has great pleasure in recording his best thanks to Professor R. S. Krishnan for his kind interest and to Dr. G. N. Ramachandran for his guidance and help throughout the investigation.

SUMMARY

The crystal structure of barium chlorate monohydrate has been completely determined. The crystals are monoclinic with space group $I2/c$-C_{2h}^6 and four molecules in a unit cell with edges $a = 8{\cdot}86$ Å, $b = 7{\cdot}80$ Å, $c = 9{\cdot}35$ Å and $\beta = 93° 26'$. The heavy atom positions were first fixed from Patterson projections and the atomic co-ordinates of all atoms were obtained from Fourier projections along the three axes. In the structure, chlorate ions retain their usual low pyramidal form. Each chlorine is surrounded by four bariums and each barium by eight chlorines. Tables are given for the various atomic co-ordinates and the interatomic distances. The structure is able to explain qualitatively the known optical properties of the crystal.

References

Beauclair, I. W. de and Sinogowitz, U.	..	"Phasenfaktoren Tafel," Akademie Verlag, Berlin, 1949.
Beevers, C. A. and Lipson, H.	..	*Nature*, 1936, **137**, 825.
Bradley, A. J.	..	*Proc. Phy. Soc.*, 1935, **47**, 879.
Buerger, M. J.	..	*X-Ray Crystallography*, John Wiley, 1942.
——— and Klein, G. E.	..	*Jour. App. Phy.*, 1945, **16**, 408.
Eakle, A. S.	..	*Z. Krist.*, 1896, **26**, 586.
Groth, P.	..	*Chemische Crystallographic*, 1908, **2**, 114.
Kartha, G.	..	*Curr. Sci.*, 1951, **20**, 151.
———	..	*Acta. Cryst.*, 1952 **5**, 549.
Lipson, H. and Beevers, C. A.	..	*Proc. Phy. Soc.*, 1936, **48**, 772.
Pauling, L.	..	*Nature of the Chemical Bond*, 1948, 346, Cornell University Press.
Robertson, J. M.	..	*Journ. Sci. Inst.*, 1943, **20**, 175.
——— and Woodward, I.	..	*Journ. Chem. Soc.*, 1940, **1**, 36.
Wilson, A. J. C.	..	*Nature*, 1942, **150**, 152.
Zachariasen, W. H.	..	*Z. Krist.*, 1929, **71**, 501, 517.
——— and Barta, F. A.	..	*Phys. Rev.*, 1931, **37**, 1626.